

Research Article

Open Access, Volume 3

Image segmentation and processing for real-time detection of oral mucosal lesions using an in-house developed fluorescence imaging device

Amar Nath Sah¹; Pavan Kumar^{2,4}; Saurav Sarkar³; Asima Pradhan^{4,5}

¹Department of Biological Sciences & Bioengineering, Indian Institute of Technology Kanpur (IITK), Kanpur 208016, India.

²Faculty of Engineering and Technology, Datta Meghe Institute of Higher Education and Research (DMIHER), Wardha, 442107, India.

³Department of All India Institute of Medical Sciences Bhubaneswar (AIIMS), Bhubaneswar, India.

⁴Department of Physics, Indian Institute of Technology Kanpur (IITK), Kanpur 208016, India.

⁵Center for Laser and Photonics (CELP), IIT Kanpur, Kanpur 208016, India.

*Corresponding Author: Asima Pradhan

Department of Physics, Indian Institute of Technology Kanpur (IITK), Kanpur 208016, India.

Email: amarnath@iitk.ac.in

Received: Mar 13, 2023

Accepted: Apr 19, 2023

Published: Apr 26, 2023

Archived: www.jclinmedimages.org

Copyright: © Pradhan A (2023).

Introduction

Objective: In the present study, detection of oral mucosal lesions using an in-house developed fluorescence imaging portable device on three groups of patients is reported. Threshold-based segmentation and image processing of fluorescence images have been executed for the identification of cancerous lesions in the affected area of oral mucosa in real time.

Methods: Fluorescence imaging measurements are performed on 11 Oral Squamous Cell Carcinoma (OSCC) patients, 19 dysplastic patients, and 22 normal volunteers. Patients having the abnormality in the buccal mucosa of oral cavity are incorporated in the presented work. A 405 nm laser diode is utilized to excite the two fluorophores i.e., Flavin Adenine Dinucleotide (FAD) and porphyrin present in the tissue. Image processing is done onto the ratio values of red (porphyrin) to green (FAD) bands by using a MATLAB based Graphical User Interface (GUI). Receiver Operating Characteristic (ROC) analysis is employed to find the sensitivity and specificity.

Results: Fluorescence images showed higher intensities of red bands than the green bands in OSCC and dysplastic patients. Segmentation carried out on the fluorescence images is seen to separate the cancerous lesion from the normal lesion in the oral mucosa. Classification tool box, based on the ratio of red to green bands was able to discriminate among the three groups with sensitivities of 95%, 84%, 95% and specificities of 97%, 86% and 84% respectively.

Conclusion: This clinical study can be utilised for the identification of margin of abnormal areas of oral mucosal lesions and thus will assist the clinician during the surgical procedure.

Keywords: Oral cancer; Fluorescence imaging; Segmentation; Image processing; Graphical user interface.

Introduction

Early detection of oral mucosal lesions is required to reduce morbidity and mortality rates. In Asian countries, especially in India, oral cancer is a concern because it is one of the topmost cancer in men (Rank 1) and in women (Rank 3) [1-3]. Among the conventional techniques, tissue biopsy with the histopathology is a reliable and accurate method. Five-year survival rate is around 45%, indicating the need to detect and diagnose the oral mucosal lesions at an early stage [4,5]. The problem with most of the cancers including oral cancer is the lack of early visible symptoms. It is therefore necessary to work on development of sensitive portable and user-friendly devices, having the potential to detect early oral carcinoma.

Optical devices have been designed for the detection of cancer by many research groups [6 -11]. Among them, fluorescence spectroscopy and imaging devices have emerged as a reliable detection tool for in vivo study of oral carcinoma [12-19]. In the fluorescence-based imaging devices, UV-visible light is generally used as an excitation source and fluorescence signal is captured by Charge Coupled Device (CCD). Diagnostic information of the fluorophores such as porphyrin, Flavin Adenine Dinucleotide (FAD), Nicotinamide Adenine Dinucleotide (NADH) is observed with 405 nm excitation wavelength with the decreasing order of intensities ($I_{\text{porphyrin}} > I_{\text{FAD}} > I_{\text{NADH}}$). Enhancement of porphyrin and reduction in FAD are found with progress of cancer. Several researchers and scientist groups have utilized fluorescence imaging systems for oral cancer detection.

Pierre M. Lane et al. group have developed a simple device for direct visualisation of oral cavity tissue fluorescence. The group utilised blue light (400 to 460 nm) for the excitation of tissue fluorophores and fluorescence signal are recorded at 470 nm [20]. A chemiluminescence based probe is developed for oral cancer detection. It involves the use of oral rinse (1% acetic acid) which helps to view the acetowhite area. This method is highly subjective and has a low sensitivity [21]. Kulapaditharom et al. utilized fluorescence endoscope for head and neck cancer detection and achieved sensitivity of 100% and specificity of 73% [22]. In a study, Betz et al. showed a clear difference between normal and malignant lesions for flat epithelial tumours than the exophytic tumours [23]. Paczona et al. noted the reduction in fluorescence intensities of green bands and shift to reddish-blue band for malignant tissues [24]. Rahman et al. obtained sensitivity of 90% and a specificity of 87% between the normal and malignant tissues by taking the ratio of red to green fluorescence [25]. In a study by Roblyer et al., the quantitative fluorescence imaging was able to differentiate the cancerous samples to normal samples with 100% sensitivity and 91.4% specificity [26].

Here, we have reported real time early diagnosis of oral mucosal lesions using an inhouse built fluorescence-based imaging device with the help of segmented images and image processing tools. Using the device, 1.0 cm² area of oral cavity lesions is captured in a single scan. Signatures of FAD and porphyrin are observed with excitation of 405 nm laser light. The intensity of red band in the fluorescence image is attributed to porphyrin

and found to increase in most of the OSCC and dysplastic patients than the normal volunteers. For classification among the groups, ROC has been employed onto the ratio ($I_{\text{porphyrin}}/I_{\text{FAD}}$). For a real-time analysis, these results are validated with a Graphical User Interface (GUI) tool.

Material and methods

Fluorescence-based imaging probe with the required accessories, while taking the measurement on a patient (carcinoma in oral buccal mucosa) are displayed in Figure 1 a & b respectively. Laser light of wavelength 405 nm (1 milliwatts incident power) is illuminated onto the oral mucosal lesion and the fluorescence signal is recorded using a charge-coupled device (CCD). At the tip of the probe, a disposable cap of teflon material is used while taking the measurements on patients and volunteers. Device fabrication and working of the probe are discussed in detail in our recently published paper [27]. Imaging measurements were performed on total 30 patients (OSCC=11, dysplastic=19) and 22 normal volunteers. Average age of the patients and volunteers with the standard deviation were 48 ± 11 , 37 ± 9 and 27 ± 7 respectively. Image segmentation and processing are done on randomly chosen an OSCC patient (45 years), a dysplastic patient (38 years) and a normal volunteer (26 years). All the relevant details, such as age, lifestyle, habits of consuming tobacco-related products etc., were noted in a questionnaire form. Ethical clearance was taken from hospital and institute (IEC communication number IITK/IEC/2015-16/2/10) for performing this clinical work.

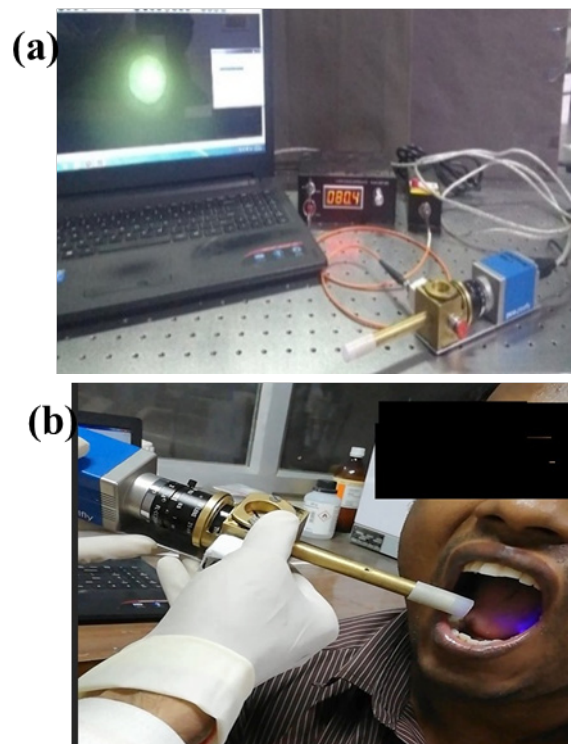


Figure 1: (a) Photographs of the fluorescence imaging device with all the accessories (laser, fluorescence device and laptop) (b) Photograph of patient taken during the fluorescence measurements.

For this clinical study, the inclusion and exclusion criteria of patient selections are shown in the flow chart (Figure 2). In the given flow chart, the overall procedure of executing the fluorescence measurements and oral biopsy are also discussed.

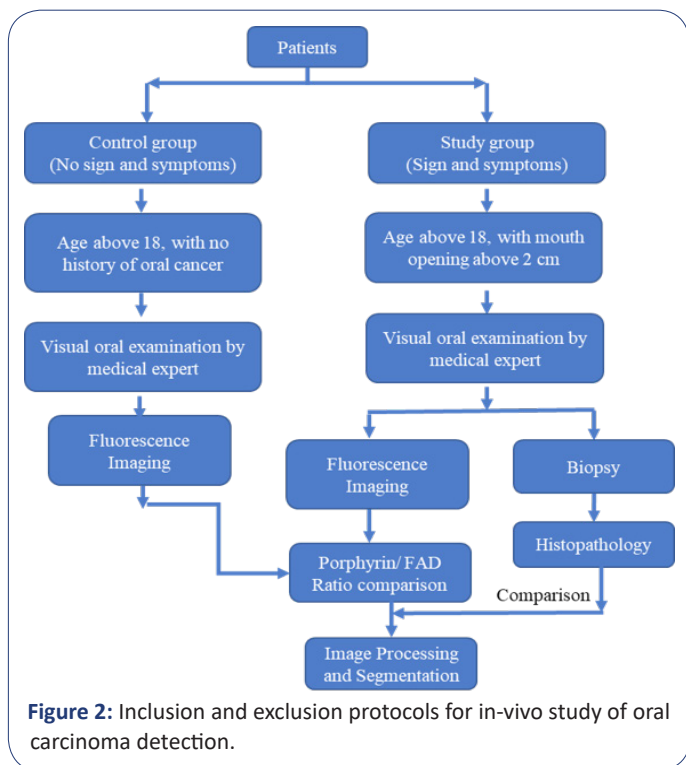


Figure 2: Inclusion and exclusion protocols for in-vivo study of oral carcinoma detection.

Results and discussion

Figure 3a displays an image of an oral mucosal patient recorded using a mobile based camera. Figure 3b is magnified image of the malignant region. The fluorescence image (real image) recorded using the imaging device is shown in figure 3c. In the image 3c, a clear contrast of red colour can be seen which is due to porphyrin.

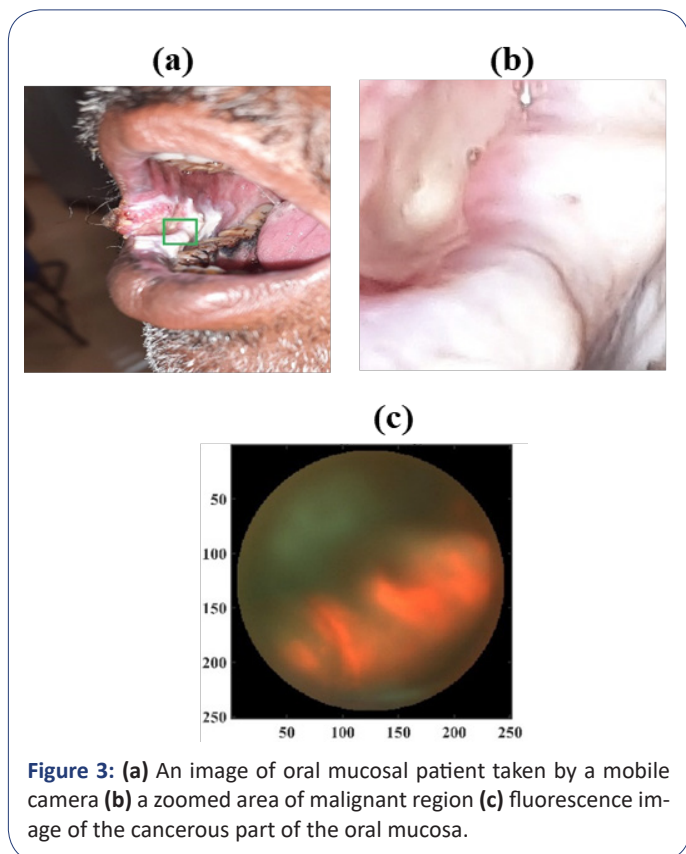


Figure 3: (a) An image of oral mucosal patient taken by a mobile camera (b) a zoomed area of malignant region (c) fluorescence image of the cancerous part of the oral mucosa.

Fluorescence image consists of red, green and blue bands. The red and green bands correspond to porphyrin and FAD respectively. Extracted images from the original image consisting of RGB bands of an OSCC patient are displayed in figure 4a-c. Figures 4a-c are red, green and blue bands of fluorescence raw image. In figure 4d & e, the ratio image of porphyrin to FAD and threshold-based segmentation of cancerous region have been shown. However, in figure 4f, abnormal segmented region is marked on the color fluorescence raw image.

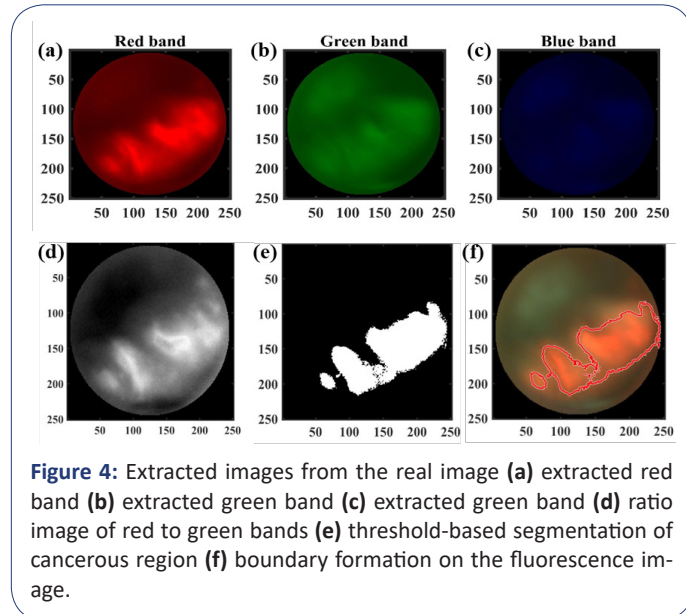


Figure 4: Extracted images from the real image (a) extracted red band (b) extracted green band (c) extracted green band (d) ratio image of red to green bands (e) threshold-based segmentation of cancerous region (f) boundary formation on the fluorescence image.

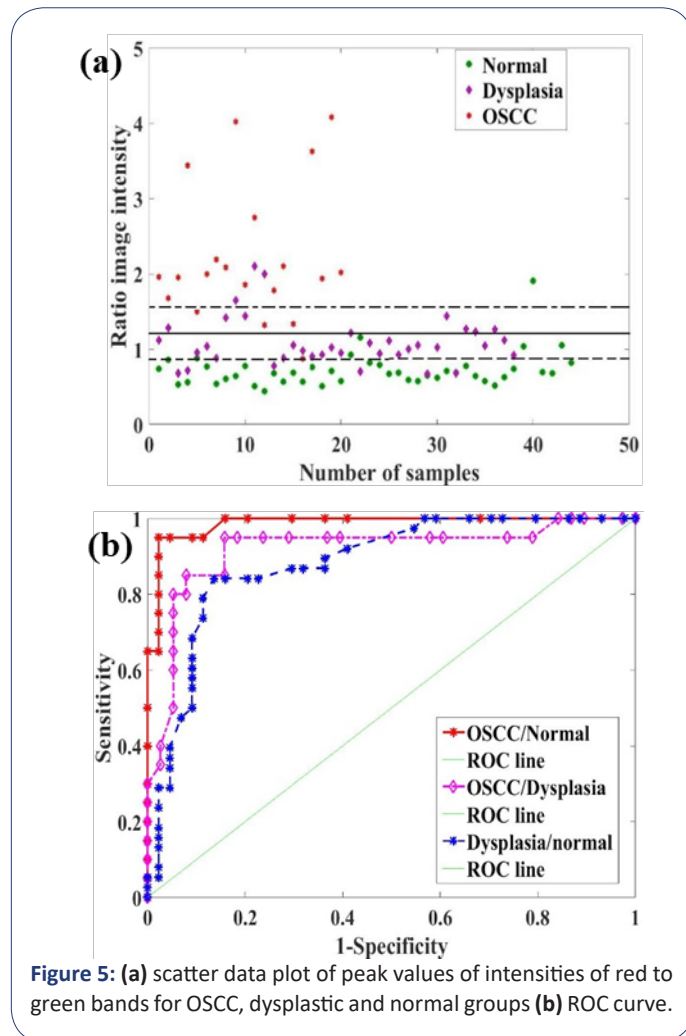


Figure 5: (a) scatter data plot of peak values of intensities of red to green bands for OSCC, dysplastic and normal groups (b) ROC curve.

A threshold-based segmentation has been performed on the ratio image to separate the malignant and normal regions. The threshold ratio values for control group are found below 0.82, for dysplastic patients, in the range from 0.82 to 1.49 and for OSCC above 1.50 using the ROC analysis. Scatter data plot along with the ROC curve are shown in figure 5. In the image shown in figure 4f, inner boundary and outer boundary formation are based on the mean errors of the threshold. This segmented image is able to accurately identify the cancerous parts of the oral mucosa.

To make the imaging technique user-friendly with real-time analysis, we developed a Graphical User Interface (GUI) panel in Matlab and its working is depicted in the figure 6. GUI has three push buttons corresponding to three images. The first pushbutton, 'select image' corresponds to the image to be analysed in the panel. The pathname and filename on GUI display the location of the oral cavity images. The raw image of the oral section taken by the probe. The second image is the R/G ratio, which displays the red to the green image ratio of the selected image. According to the ratio value, analysed results will be displayed. The third push button i.e., Segmented image shows the boundaries around the cancerous region. Analysis performed on OSCC, dysplastic (precancer) and normal groups are displayed in figure 6 a-c.

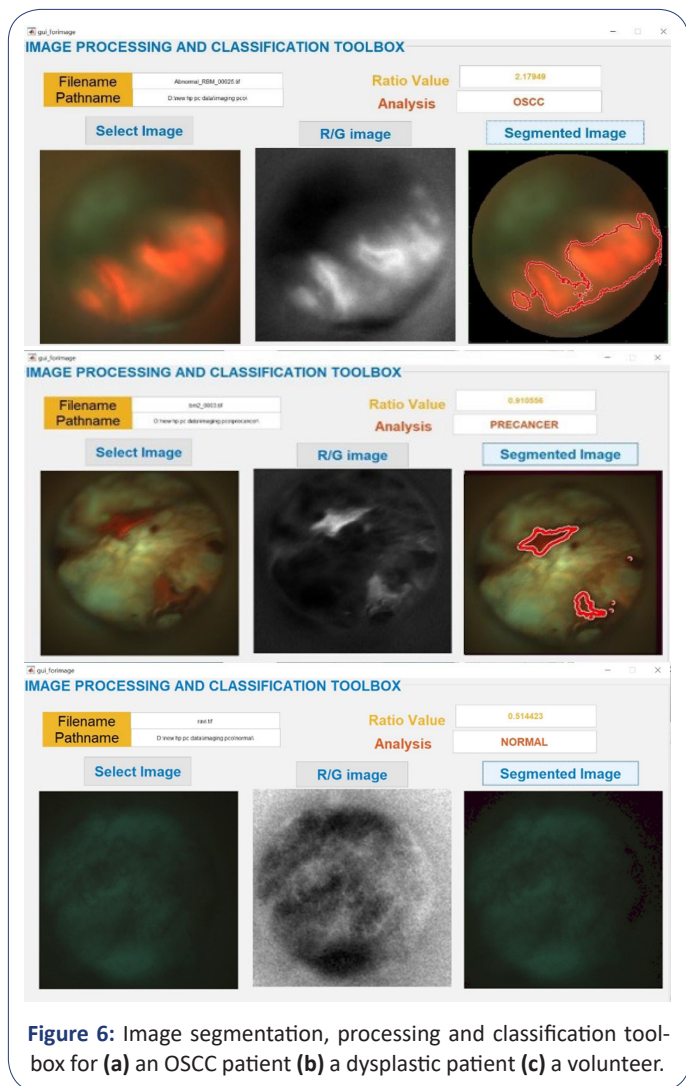


Figure 6: Image segmentation, processing and classification toolbox for (a) an OSCC patient (b) a dysplastic patient (c) a volunteer.

Conclusion

In the clinical study, detection of oral mucosal lesions using the fluorescence-based imaging technique, segmentation and image processing tools were carried out. With 405 nm laser light, fluorescence due to FAD and porphyrin were observed. Porphyrin contribution was found to be higher in OSCC and dysplastic patients than in the normal volunteers. Segmentation carried out on the fluorescence images demarcate the most affected region of the oral mucosal lesion. GUI was able to classify among the groups based on ratio values and segmentation. In conclusion, the minimally invasive optical technique coupled with an objective analysis method (toolbox) can be an efficacious method for early detection of oral mucosal lesions of different grades.

Acknowledgements: Authors are very much thankful to Dr. Surendra Kumar Kanujia for providing samples in initial study.

References

1. Ferlay J, Soerjomataram I, Dikshit R, Eser S, Mathers C, et al. Cancer incidence and mortality worldwide: sources, methods and major patterns in globocan. *International journal of cancer*. 2015; 136: 359-386.
2. Omar E. Current concepts and future of noninvasive procedures for diagnosing oral squamous cell carcinoma-a systematic review. *Head Face Med*. 2015; 11.
3. El-Naggar AK, Chan JKC, Takata T, Grandis JR, Slootweg PJ. The fourth edition of the head and neck World Health Organization blue book: editors' perspectives. *Human pathology*. 2017; 66: 10-12.
4. Scully C, Bagan JV, Hopper C, Epstein JB. Oral cancer: Current and future diagnostic techniques. *Am J Dent*. 2008; 21: 199-209.
5. Koenig K, Schneckenburger H. Laser-induced autofluorescence for medical diagnosis. *J Fluoresc*. 1994; 4: 17-40.
6. Tromberg BJ, Shah N, Lanning R, Cerussi A, Espinoza J, et al. Non-invasive in vivo characterisation of breast tumours using photo migration spectroscopy. *Neoplasia*. 2000; 2: 26-40
7. Hillemanns P, Reiff J, Stepp H, Soergel P. Lymph node metastasis detection of ovarian cancer by porphyrin fluorescence photodetection: case report. *Lasers Med Sci*. 2007; 22: 131-135.
8. De Veld DC, Bakker Schut TC, Skurichina M, Witjes MJ, Van der Wal JE, et al. Autofluorescence and Raman microspectroscopy of tissue sections of oral lesions. *Lasers Med Sci*. 2005; 19: 203-209
9. Bergholt MS, Zheng W, Lin K, Ho KY, Teh M, et al. Combining near-infrared-excited autofluorescence and Raman spectroscopy improves in vivo diagnosis of gastric cancer. *Biosens Bioelectron* 2011; 26: 4104-4110.
10. Alfano RR. Advances in ultrafast time resolved fluorescence physics for cancer detection in optical biopsy. *AIP Advances*. 2012; 2: 011103.
11. DeCoro M, Wilder-Smith P. Potential of optical coherence tomography for early diagnosis of oral malignancies. *Expert Rev Anticancer Ther*. 2010; 10: 321-329.
12. De Veld DC, Witjes MJ, Sterenberg HJ, Roodenburg JL. The status of in vivo autofluorescence spectroscopy and imaging for oral oncology. *Oral Oncol*. 2005; 41: 117-131.
13. Farwell DG, Meier JD, Park J, Sun Y, Coffman H, et al. Time-resolved fluorescence spectroscopy as a diagnostic technique of oral carcinoma. *Arch Otolaryngol Head Neck Surg*. 2010; 136:

-
- 126-133.
14. Amelink A, Sterenborg HJ, Roodenburg JL, Witjes MJ. Noninvasive measurement of the microvascular properties of non-dysplastic and dysplastic oral leukoplakias by use of optical spectroscopy. *Oral Oncol.* 2011; 47:1165-1170.
 15. Poh CF, Zhang L, Anderson DW, Durham JS, Williams PM, et al. "Fluorescence visualisation detection of field alterations in tumor margins of oral cancer patients," *Clinical Cancer Research.* 2006; 12: 6716-6722.
 16. Kumar P, Singh A, Kanaujia SK, Pradhan A. Human saliva for oral precancer detection: a comparison of fluorescence & stokes shift spectroscopy. *J Fluoresc.* 2018; 28: 419-426.
 17. Kumar P, Kanaujia SK, Singh A, Pradhan A. In vivo detection of oral precancer using a fluorescence-based, in-house-fabricated device: a Mahalanobis distance-based classification, *Lasers Med Sci.* 2019; 34: 1243-1251.
 18. Gillenwater A, Jacob R, Ganeshappa R, Kemp B, El-Naggar AK, et al. Noninvasive diagnosis of oral neoplasia based on fluorescence spectroscopy and native tissue autofluorescence. *Arch Otolaryngol Head Neck Surg.* 1998; 124:1251-1258.
 19. Betz CS, Mehlmann M, Rick K, Stepp H, Grevers G, et al. Autofluorescence imaging and spectroscopy of normal and malignant mucosa in patients with head and neck cancer. *Lasers Surg Med.* 1999; 25: 323-334.
 20. Lane PM, Gilhuly T, Whitehead P, Zeng H, Poh C, et al. Simple device for the direct visualisation of oral-cavity tissue fluorescence, *J Biomed Opt.* 2006; 11:024006.
 21. Onizawa K, Okamura N, Saginoya H, Yoshida H. Characterisation of autofluorescence in oral squamous cell carcinoma. *Oral Oncol.* 2003; 39: 150-156.
 22. Betz CS, Stepp H, Janda P, Arbogast S, Grevers G, et al. A comparative study of normal inspection, autofluorescence and 5-ALA-induced PPIX fluorescence for oral cancer diagnosis. *Int J Cancer.* 2002; 97: 245-252.
 23. Paczona R, Temam S, Janot F, Marandas P, Luboinski B. Autofluorescence videoendoscopy for photodiagnosis of head and neck squamous cell carcinoma. *Eur Arch Otorhinolaryngol.* 2003; 260: 544-548.
 24. Rahman MS, Ingole N, Roblyer D, Stepanek V, Richards-Kortum R, et al. Evaluation of a low-cost, portable imaging system for early detection of oral cancer. *Head Neck Oncol.* 2010; 2: 10.
 25. Roblyer D, Kurachi C, Stepanek V, Williams MD, El-Naggar AK, et al. Objective detection and delineation of oral neoplasia using autofluorescence imaging. *Cancer Prev Res (Phila).* 2009; 2: 423-431.
 26. Sah AN, Kumar P, Pradhan A. In vivo testing of oral mucosal lesions with in-house developed portable imaging device and comparison with the spectroscopy results. *J of Flu.* 2023; 26: 1-9.